Atmos. Chem. Phys. Discuss., 12, 16557–16602, 2012
www.atmos-chem-phys-discuss.net/12/16557/2012/
doi:10.5194/acpd-12-16557-2012

Atmospheric Chemistry and Physics Discussions

Measurements and modelling of ozone in the Mediterranean MBL: an investigation of the importance of ship emissions to local ozone production

I. M. Hedgecock[1], **C. N. Gencarelli**[1,2], **G. J. Schürmann**[1,*], **F. Sprovieri**[1], and **N. Pirrone**[1]

[1]Institute for Atmospheric Pollution Research, Rende Section, Rende, 87036, Italy
[2]Department of Physics, University of Calabria, Arcavacata di Rende, 87036, Italy
[*]now at: Max Planck Institute for Biogeochemistry – Biogeochemical Systems Department, P.O. Box 10 01 64, 07701 Jena, Germany

Received: 3 May 2012 – Accepted: 11 June 2012 – Published: 5 July 2012

Correspondence to: I. M. Hedgecock (i.hedgecock@iia.cnr.it)

Published by Copernicus Publications on behalf of the European Geosciences Union.

Abstract

Elevated concentrations of ground level ozone are both hazardous to human health and detrimental to agricultural production. The Mediterranean Basin, due to its position under the descending branch of the Hadley Cell circulation during the summer months, enjoys periods of stable, sunny and warm weather which provide ideal conditions for the production of ozone. The presence of major population centres and numerous industrialised areas in the coastal zone result in both a continual supply of ozone precursor compounds and also a significant number of people to suffer the consequences of high ozone concentrations. Using the WRF/Chem model validated with data obtained from seven oceanographic measurement campaigns, performed between 2000 and 2010, aboard the Italian Research Council's R. V. Urania, and also from a number of EMEP monitoring stations located around the Mediterranean Basin, the importance of emissions from maritime traffic in the region has been investigated. The model results indicate that over large areas of the Mediterranean emissions from shipping contribute between 5 and 10 ppb to the ground level O_3 daily average concentration during the summer. The contribution to the hourly average O_3 is up to 40 ppb in some particularly busy shipping lanes. Importantly the results suggest that in a number of coastal areas the contribution from ship emissions to the local O_3 concentration can make the difference between complying with the EU Air Quality standard of a maximum 8 h mean of 120 $\mu g\,m^{-3}$ and exceeding it.

1 Introduction

Measurements of ozone at numerous locations in the Mediterranean Basin have all shown that the region experiences significantly higher levels of boundary layer ozone than European background sites. The region also experiences episodes during which ozone concentrations reach and remain at levels which exceed EU standards and are considered harmful for human health, and which also have a detrimental effect on

ACPD
12, 16557–16602, 2012

vegetation and agriculture. These elevated concentrations of O_3 have been observed at coastal sites (Nolle et al., 2002; Saliba et al., 2008; Gerasopoulos et al., 2005), inland sites (see Cristofanelli and Bonasoni, 2009, and references therein), during intensive field campaigns (for example Lelieveld et al., 2002), and also over the sea itself as shown by measurements performed on board a cruise liner over two summers (Velchev et al., 2011), and on board the Italian Research Council's R. V. Urania as described here.

The Mediterranean Basin is conducive to the production of elevated levels of O_3 for both geographical and meteorological/climatological reasons. During the summer the Mediterranean is under the descending arm of the Hadley circulation, leading to prolonged periods of stable, warm and sunny weather, which favours both O_3 formation and the natural production of VOC (Millán et al., 2002). In the Western Basin the formation of diurnal recirculation patterns between the land and the sea mean that O_3 rich air produced over land during the day is moved over the sea in the evening, where it is effectively stored over night. In the morning the onshore breeze carries that same air back over land, where it can continue to accumulate precursors and produce more O_3 (Millán et al., 2002; Adame et al., 2009).

The recirculation phenomena seems to be more important in the Western Basin than the Eastern (see Velchev et al., 2011, and references therein), both the Eastern and Western Basins of the Mediterranean are influenced by the outflow of polluted air masses from more central and northern parts of Europe (Lelieveld et al., 2002; Kalabokas et al., 2007, 2008; Cristofanelli and Bonasoni, 2009). The eastern region of the Mediterranean is also becoming more influenced by increasing urbanization, the growth of Istanbul and Cairo being the most obvious examples (Kanakidou et al., 2011; Im and Kanakidou, 2011). The transport of polluted air from Central to Northern Europe has been implicated in air quality exceedances in North Africa and the Middle East (Duncan et al., 2008), while trans-Atlantic transport of polluted air from North America appears to influence O_3 concentrations in the free troposphere over the Mediterranean (Lelieveld et al., 2002; Auvray and Bey, 2005; Cristofanelli and Bonasoni, 2009).

ACPD
12, 16557–16602, 2012

Ozone produced in the boundary layer can be advected upwards to the free troposphere, for example polluted air from the Po Valley in Italy has regularly been detected on Monte Cimone in the Apennines (Bonasoni et al., 2000; Cristofanelli et al., 2007; Cristofanelli and Bonasoni, 2009). Increased O_3 in the free troposphere over the Mediterranean is of interest because its efficacy as a greenhouse gas is greater in the free troposphere than it is in the boundary layer; generally speaking the capacity of O_3 to trap heat in the atmosphere increases from the ground to the tropopause (Worden et al., 2011). The impact of regional climate change on O_3 concentrations in the Mediterranean region has also been investigated recently, with a particular focus on the Eastern Mediterranean, where the rapid growth of a number of population centres and the envisaged increase in temperature in a future climate (particularly in summertime), has led to some concern over future air quality. Im and Kanakidou (2011) have performed a series of air quality modelling studies in which the effect of temperature perturbations have been investigated. The authors found an increase of approximately 1 ppb in the O_3 concentration with each 1 K rise in temperature. The Mediterranean has been identified as a regional hot spot in terms of air quality (Monks et al., 2009), and is a region that has been identified as susceptible to climate change, the probable future summer time temperature increase, will have repercussions for both atmospheric composition and the hydrological cycle (IPCC, 2007).

In addition to the characteristics described above the Mediterranean is one of the busiest shipping routes in the world. Emissions from shipping have been coming under increasing scrutiny over the last several years (Eyring et al., 2005, 2007, 2010; Marmer and Langmann, 2005; Corbett et al., 2007; Matthias et al., 2010; Miola and Ciuffo, 2011). The impact of shipping emissions is expected in to increase in magnitude as global maritime traffic increases, and in relative importance as legislation regulating emissions from terrestrial industry and transportation becomes increasingly strict, and widely applied. The environmental consequences of ship emissions can be numerous; the particulate matter directly emitted has consequences for human health (Corbett et al., 2007), SO_2 emissions can lead to sulphate particle formation, which can have

ACPD
12, 16557–16602, 2012

a cooling effect on climate, while the black carbon emitted can have the opposite effect. NO_x emissions can locally titrate O_3, but after being dispersed lead to enhanced O_3 production in coastal areas (Vutukuru and Dabdub, 2008; Song et al., 2010). Ship emissions can also lead to acidification and eutrophication via nitrate deposition to coastal waters and land (Derwent et al., 2005; Dalsøren et al., 2009). The role ship emissions play in tropospheric photochemistry and the methodologies to include them in Chemical Transport Models (CTMs) is discussed in more detail in Sect. 3.2.1.

The major ports and shipping lanes in the Mediterranean are easily identified in NO_x or SO_x emissions maps of the region and clearly represent a major emission source in the region, with hot spots through the Strait of Gibraltar, the Strait of Sicily, the Adriatic and Ligurian Seas and the entrances to the Black Sea and the Suez Canal. During an almost annual series of oceanographic campaigns aboard the Italian Research Council's Research Vessel, the R. V. Urania, O_3 measurements were performed as a complement to the primary research aim of these campaigns, which was the determination of Hg species concentrations in the Marine Boundary Layer (MBL), and usually also in the water column, see Sect. 2.2. While modelling Hg for one particular campaign (in the Adriatic in the summer of 2005, Sprovieri et al., 2010), it was observed that over the whole of the period during which O_3 measurements were made, from the 17 June till the 29 June, the average O_3 concentration was slightly over 60 ppb. The WRF/Chem model (version 3.1) (Grell et al., 2005), was used to simulate atmospheric chemistry for the campaign period to investigate the impact which ship emissions might have on the concentration of O_3 along the route of the R. V. Urania. These preliminary studies suggested that up to 20 % of the O_3 in the boundary layer could be due to shipping emissions of NO_x. That study has now been extended to include the oceanographic campaigns performed over different routes in the Mediterranean in 2000, 2003, 2004, 2006, 2009 and 2010. The simulations used a nested grid of 9 km by 9 km to cover the area traced by the R. V. Urania, while the largest of the three domains covered most of Europe, the Mediterranean, parts of North Africa and the Middle East. Emissions were taken from the EMEP (European Monitoring and Evaluation Programme) database

ACPD
12, 16557–16602, 2012

and interpolated into the three domains, see Sects. 3.1.1 and 3.2. Simulations were performed using all emission sectors, and both the meteorological and the O_3 concentration results were compared to the observations made aboard the R. V. Urania, and to those taken at EMEP stations located in the highest resolution modelling domain. The same simulations were then run again with the shipping emissions removed and the results compared. The results imply that emissions from ships have a significant influence on O_3 concentrations over much of the Mediterranean, and a major influence close to busy shipping routes.

2 Measurements

2.1 Measurements aboard the R. V. Urania

Ozone concentrations were measured using a Teledyne–API model 400A UV ozone analyser. The analyser was calibrated every 24 h using an internal permeation source, and employing a sampling flow rate of 0.8 l min^{-1}, over a five minute period gave a detection limit of 0.6 ppb. The same instrument has been used on all the oceanographic campaigns to date. The R. V. Urania is equipped with an automated weather station which is approximately 30 m above the sea surface. Of most interest to the validation were the temperature, humidity, wind speed and direction data which were available at five minute intervals.

2.2 The Med-Oceanor Series of oceanographic campaigns

The Med-Oceanor oceanographic campaigns are part of a continuing series of almost yearly research cruises aboard the R. V. Urania, which began in 2000. Their primary aim has been to investigate Hg cycling in the Mediterranean boundary layer, surface water, the water column, sediments and the exchange of Hg species between the water and the atmosphere (Sprovieri et al., 2003; Andersson et al., 2007; Kotnik et al., 2007;

ACPD
12, 16557–16602, 2012

Ferrara et al., 2003; Gårdfeldt et al., 2003). However as well as Hg species, a number of gas and aerosol phase atmospheric species have been measured each year.

The Med-Oceanor campaign in 2000 took place between 14 July and 8 August, the route took in the Tyhrennian Sea around Sardinia, skirted Sicily and went to the south-east of Crete in the Eastern Basin. The 2003 campaign (between 5 and 27 August) was the most wide ranging of the campaigns to date; the cruise route went as far as the south of Crete in the East and almost to the Strait of Gibraltar in the west. The campaign in 2004 is the only campaign so far which has taken place in the springtime, (18 March to 3 April).

The intention of the Med-Oceanor 2005 (15 June till 5 July) was to investigate Hg in the Adriatic atmosphere, water column and sediments. It was during this cruise that the average O_3 concentration over the whole period was slightly over 60 ppb (Sprovieri et al., 2010). The campaign in 2006 (5–20 July) went further East than the previous campaigns, the route passed to the south of Crete and reached the area north of the Nile Delta. High pressure over Central Europe resulted in conditions favourable to ozone production and the O_3 concentrations were again high during this campaign. The 2009 (7–30 June) campaign stayed mostly in Italian coastal waters, predominantly in the Tyhrennian but also passed south into the Ionian Sea. The 2010 campaign ran from 27 August until 12 September, it followed the Italian coast south from Naples, went into the Gulf of Taranto and then East towards Crete before returning to Palermo via the Strait of Sicily. The routes are shown in Fig. 1.

2.3 Observations from the EMEP Network

Data from the EMEP network of monitoring sites have been used for the validation of both the meteorological and chemistry output from the WRF/Chem model.The EMEP stations chosen were those located in the highest resolution modelling domain, the positioning of which varied with the cruise path of the year in question, see Sect. 3.1.1.

ACPD
12, 16557–16602, 2012

3 Modelling

3.1 The model setup

3.1.1 Modelling domains

The first modelling domain of 66 by 66 grid cells (81 km by 81 km resolution centred at 51° N and 13° E), covers an area from the edge of Greenland, includes all of Scandinavia, and extends as far south as the northern part of the Red Sea and to the East beyond the Black Sea, see Fig. 2. The intermediate domain has a resolution of 27 km by 27 km and was chosen according to the cruise route in such a way to provide an adequate number of grid cells between its boundaries and the inner (9 km by 9 km) domain, which was chosen to cover the area taken in by the campaign as shown in Fig. 2. Twenty-eight vertical levels up to 5000 Pa were used for all three domains in all the simulations.

3.1.2 Physics

The non-hydrostatic mesoscale chemical transport model WRF/Chem offers a number of parametrisation options to represent the physical processes which take place in the atmosphere. A detailed description of these can be found in Skamarock et al. (2008), those used in this modelling study are as follows. The Purdue-Lin scheme was used for microphysics, it includes six classes of hydrometeors (water vapour, cloud water, rain, cloud ice, snow and graupel), the Mellor-Yamada-Janjic (MYJ) scheme was used for the Planetary Boundary Layer (PBL) parametrisation, this scheme describes vertical sub-grid-scale fluxes due to eddy transport in the whole atmospheric column, while the horizontal eddy diffusivity is calculated with a Smagorinsky 1st order closure. The surface layer parametrisation employed was the Eta surface layer scheme (it is based on similarity theory), the land surface model to describe interactions between the soil and atmosphere was Noah LSM (4 soil layers), the Kain-Fritsch scheme was used for

ACPD
12, 16557–16602, 2012

cumulus parametrisation and the Rapid Radiative Transfer Model (RRTM) and Dudhia schemes for long and shortwave radiation, respectively. The period of the 2005 oceanographic campaign was simulated repeatedly using different combinations of parametrisations to assess how the choice influenced both model output and simulation time. The combination described above proved to be the most appropriate for the studies performed. It should be pointed out that the simulations performed in this study apply specifically to the Mediterranean summer and that the combination of parametrisations above may not be ideal in other cases.

3.1.3 Chemistry

The RADM2 (Regional Acid Deposition Model, version 2) mechanism (Stockwell et al., 1990) and the Madronich photolysis scheme (Madronich, 1987) were used in all the simulations. The photolysis rate constants were recalculated every 30 min.

3.1.4 Input data and Initialisation

The meteorological input data, obtained from the Research Data Archive (RDA), were the NCEP FNL (final) Global Operational Analyses, which are provided on a 1° by 1° grid at six hourly intervals. The data are converted to WRF input on the appropriate domain(s) using the WRF Preprocessing System (WPS). The chemical species concentrations were initialised using the idealised profile in WRF/Chem (chem_in_opt = 0), and the model was allowed to spin-up for five days before the beginning of the observation period under study.

3.2 Emissions

The WRF/Chem model includes the option to calculate biogenic emissions on-line using the approach described by Guenther et al. (1993, 1994) and Simpson et al. (1995). During the simulations the biogenic emission fluxes were up-dated every 30 min. The anthropogenic emissions used in the model were obtained from the EMEP Centre for

ACPD
12, 16557–16602, 2012

Emission Inventories and Projections (CEIP) (http://www.ceip.at/). The emissions used in EMEP models (Vestreng et al., 2007) for the years corresponding to the measurement campaigns were used. As in Schürmann et al. (2009) a day-night temporal profile has been applied to the emissions following Simpson et al. (2003). The EMEP emissions were preferred because of their specificity to the Europe/Mediterranean region, their availability for individual years, and also the results obtained by Marmer et al. (2009) in a comparison of shipping emission inventories for the Mediterranean Sea. Marmer et al. (2009) found that in their modelling study, at least in the Western Basin, the EMEP inventory gave the best match with the major part of the measurements with which they compared their simulations.

3.2.1 In-plume chemistry and artificial plume dilution

The perturbation caused by ship emissions to local photochemistry in the MBL, and their possible impact began to be investigated in detail in the late 90s (Lawrence and Crutzen, 1999; Capaldo et al., 1999). The chemistry of ship plumes has been studied using Lagrangian models (Song et al., 2003; von Glasow et al., 2003), and the problem of accurately representing plume chemistry in Eulerian models has also been studied (Charlton-Perez et al., 2009; Huszar et al., 2010). The inclusion of ship emissions in Chemical Transport Models (CTMs) results in the instantaneous dilution of the emissions within the volume of the grid cell. In coarse resolution models this leads a to a false impression of the chemical composition in the cell, because the chemistry which occurs within the volume of the expanding plume, where the chemical composition is different to the air in the rest of the cell, is not taken into account (see Charlton-Perez et al., 2009; Huszar et al., 2010; Vinken et al., 2011). This can lead to errors in the simulation of NO_x and OH concentrations and in the simulated ozone production efficiency (OPE) (Charlton-Perez et al., 2009). Clearly in all atmospheric modelling simulations which include emissions from point sources this artificial dilution occurs, however, often stationary sources are co-located in urban/industrial zones where the abundance of sources will tend to lead to a less pronounced dilution effect. A recent study of the effect

ACPD
12, 16557–16602, 2012

of including non-linear chemistry for ship emissions in the GEOS-Chem model (Vinken et al., 2011) indicates that the impact of dilution is less significant over more heavily polluted areas such as the North Sea, than it is in more pristine and remote areas of the MBL. The reduction made by their ship plume chemistry parametrisation to the modelled O_3 concentration was between 10 and 50 % over the North Atlantic, but only 3 % over the North Sea. Huszar et al. (2010) found that including a ship plume parametrisation into a regional CTM reduced O_3 production due to ship emissions by 15–30 % (≈4–6 ppb) over coastal areas of Europe. The model resolution clearly plays a role in the extent to which emissions are diluted, this has been investigated by Charlton-Perez et al. (2009) who estimated from their high resolution studies that a CTM using 5° by 5° resolution using instant dilution of ship emissions would overestimate O_3 production by almost 60 %. Another aspect of plume emissions from shipping which has been considered recently in the literature is the influence on plume dilution resulting from the combination of boundary layer convection, the plume's buoyancy – it is hotter than the surrounding air – and the ship's speed and direction relative to the wind speed and direction (Chosson et al., 2008). These factors influence both plume rise, which can be 2–10 times the actual stack height, and the shape of the plume (Chosson et al., 2008 and references therein). Chosson et al. (2008) also point out that the boundary layer structure has a strong influence on plume rise and the rate of plume dilution.

3.3 The simulations performed

The model resolution employed over the route taken by the R. V. Urania is 9 km by 9 km, while the resolution of the emissions database is 50 km by 50 km. Thus the introduction of the emissions into a model cell is different to most of the cases described in Sect. 3.2.1 where relatively highly spatially resolved emissions are diluted in to a coarse resolution horizontal grid. The approach used here follows that of Huszar et al. (2010) where the emissions from the EMEP database are distributed among the model cells. Although Mediterranean shipping travels in relatively well defined shipping lanes, these are obvious wide for safety reasons, and contain a large number of ships at any one

ACPD
12, 16557–16602, 2012

time, given that the density of Mediterranean maritime traffic is among the highest in the world. Shipping lanes also clearly occur in pairs with ships travelling in either direction. (The website http://www.marinetraffic.com/ais/ gives a real time insight into the number and position of ships. The congestion in the Strait of Sicily, the Strait of Gibraltar and the Gulf of Genoa are clear). Given these considerations, in this study the EMEP emissions have been directly interpolated on to the model grid. Two emission height cases have been investigated for the shipping emissions to assess the importance of plume rise on the modelling results. In the EMEP unified model all emissions from SNAP (Selected Nomenclature for Air Pollution) sector 8 (other mobile sources and machinery, which includes shipping) are assumed to be emitted in the first model layer (0–92 m). The WRF/Chem simulations described here, given the synoptic conditions prevailing during the periods of the oceanographic campaigns investigated, generally had 5 vertical levels from sea level to roughly 400 m a.s.l. over the open Mediterranean. This is a fairly typical height of the Mediterranean MBL under summertime anticyclonic conditions. To determine how plume rise might influence the modelling results, two emission scenarios have been simulated. In the first the emissions are emitted into the first model level (Em_low scenario) and in the second simulations were performed in which it was assumed that emissions occurred in model levels 2 (≈30–90 m, 50 %), 3 (≈90–160 m 25 %) and 4 (≈160–250 m, 25 %), the Em_hi scenario.

Simulations to estimate the impact of ship emissions on O_3 production were performed using a modified version of the emissions database, in which all emissions from SNAP sector 8 which coincided with model cells that were over the sea were removed. This was achieved using the ISO 2 (country/area code) entry in the EMEP database and removing all the SNAP sector 8 entries for the area "MED".

In order to investigate the possibility that the use of nudging might improve the quality of the comparison between the model and the observations the Em_hi simulations were repeated using the applying the WRF nudging option for temperature, relative humidity and wind. The forcing was applied every six hours and the nudging coefficients were $0.0003\,s^{-1}$. The use of the nudging option did not actually improve the quality of the

ACPD
12, 16557–16602, 2012

comparison between the measurements and observations to any great extent, for either meteorological parameters or O_3 concentrations, and in some cases it worsened. The one significant exception was for the campaign performed in 2006, as discussed in Sect. 4.1.2.

4 Results and discussion

4.1 Model validation

The ability of the WRF/Chem modelling system to reproduce measured meteorological parameters and ozone concentrations has been assessed using measured data from the Med-Oceanor series of campaigns and data from the EMEP measurement stations present in the Mediterranean region. The comparison with EMEP data has been performed taking into account those stations located within the smallest modelling domain for each of the simulation periods. The comparison between measurements and model output was made using the metrics listed in Table 1 as they are defined in Chang and Hanna (2004) and Willmott et al. (1985), where X_{mod} and X_{obs} are the modelled and observed values respectively, σ is the standard deviation and N the number of pairs. The bias indicates the over or underestimation of the parameter in question in the units of the measurement. The root mean square error provides a measure of the model precision, and can be divided in to two parts, the systematic and unsystematic. The linear bias produced by a model is described by the systematic part of the RMSE, RMSE_s Willmott et al. (1985); in Tables 2, 3 and 4 the unsystematic fraction of the RMSE is given, derived from:

$$\mathrm{RMSE}^2 = \mathrm{RMSE}_u^2 + \mathrm{RMSE}_s^2 \text{ (Willmott et al., 1985).} \quad (1)$$

The unsystematic fraction (UF) of the RMSE in Tables 2 and 3 can take values between 0 and 1. The Index of Agreement, as its name implies is a measure of the degree of

ACPD
12, 16557–16602, 2012

agreement between the model and the observations and it too can also have values between 0 and 1, with 1 indicating perfect agreement.

4.1.1 Meteorological parameters

The performance statistics for the comparison between the modelled and measured hourly values of temperature (°C), wind speed ($m\,s^{-1}$) and relative humidity (%) are shown in Table 2. The relative humidity is calculated from the model output, water vapour $kg\,kg_{air}^{-1}$ as described in Wallace and Hobbs (1977) using the vapour pressure definition from Lowe (1977). It should be noted that the calculation of the relative humidity requires the use of model output parameters, the temperature and pressure, which are themselves subject to uncertainty.

The quality of the comparison between the modelled and measured meteorological parameters is similar to results previously obtained using the WRF model (see for example Grell et al., 2005; de Meij et al., 2009; Misenis and Zhang, 2010; Schürmann et al., 2009; Tie et al., 2007; Tuccella et al., 2012). The values for the RMSE of the wind speed are however generally somewhat higher than found in previous studies with values between 3.05 and 4.66 $m\,s^{-1}$, whereas it is more commonly around 2 $m\,s^{-1}$ in the studies mentioned above. There are two main reasons for this, the first is the generally anticyclonic meteorological conditions which prevailed during the cruise campaigns, when the wind speed is often very low; the average wind speed during the whole series of Med-Oceanor oceanographic campaigns was around 6 $m\,s^{-1}$. Low wind speeds are common in the Mediterranean region during the summer anticyclone and they prove difficult to model accurately, (see de Meij et al., 2009 and references therein). The other common difficulty encountered in modelling the wind speed (and direction) in the Mediterranean is due to the very localised local circulation patterns which occur due to the complex orography near the coastline, as described in Sect. 1.

The 2003 campaign encountered some technical difficulties with the meteorological data collection during its second half which followed a route from Naples almost to the Strait of Gibraltar and returned to Livorno, and this had an impact on the quality of the

ACPD
12, 16557–16602, 2012

overall comparison. Therefore only the first part of the campaign is considered, that is from 5–16 August, in the validation of the meteorological variables obtained aboard the R. V. Urania, the whole period (up to 27 August) is considered however for the comparison with the EMEP station data.

During the 2005 Med-Oceanor campaign in the Adriatic the temperature is significantly underestimated. A closer look at the temperature data revealed that this occurred when the R. V. Urania entered the Adriatic Sea itself. The mean bias between the modelled and measured sea surface temperature for most of the campaigns is less than 1.5 °C, and for the first part of the 2005 campaign, prior to entering the Adriatic the mean bias in SST was 0.7 °C. However during the Adriatic part of the campaign the it was 3.7 °C, and this affected the simulated temperature. However this did not seem to have a major effect on the modelled O_3, which compared well to the observations, see Sect. 4.1.2.

4.1.2 Ozone

Comparisons of modelled and measured ozone concentrations have been performed for the data obtained during the oceanographic campaigns, and also with measured ozone concentration data from stations in the EMEP monitoring network located within the smallest modelling domain, for each of the years (Hjellbrekke et al., 2011). The agreement between the modelled concentrations and the observations are on a par with those from a number of previous studies. A number of studies of ozone using WRF/Chem have been performed (for example, for regions in the US: Grell et al., 2005; Fast et al., 2006; Hu and Zhang, 2006; Zhang, 2008; Misenis and Zhang, 2010; Mexico City: Tie et al., 2007; Zhang and Dubey, 2009; and for regions in Europe: Schürmann et al., 2009; de Meij et al., 2009; Tuccella et al., 2012; and also in China: Geng et al., 2007). A summary of the statistical measures to assess the model's performance in reproducing the observations during the oceanographic measurement campaigns is presented in Table 3. The table includes the results from the two emission scenarios Em_hi and Em_low mentioned in Sect. 3.2.1, the differences between these are

ACPD
12, 16557–16602, 2012

discussed further in Sect. 4.2, however as can be seen from Table 3 the difference in the results in the first model layer are not very large. The model does not consistently over or underestimate the ozone concentrations, the bias in some years is negative and others positive. Generally the model reproduces the measured O_3 concentrations reasonably well, although some campaigns were however reproduced less well than others. As mentioned in Sect. 4.1.1 the second half of the 2003 measurement campaign encountered some technical difficulties, and the comparison between the measured and modelled meteorological values was performed only for the first half of the campaign. For consistency the values in Table 3 refer to the first part of the campaign from 5–16 August.

It is interesting to note however that the O_3 concentrations observed during the second period of the 2003 campaign (Naples – the Strait of Gibraltar – Livorno) were some of the lowest recorded during the series of Med-Oceanor campaigns, and on a number of occasions were below 30 ppb. It is probable that given the vicinity of the route to major shipping lanes that the measurements were directly influenced by fresh emission plumes from the large amount of maritime traffic. Enhanced local levels of NO would reduce the O_3 concentration via reaction to form NO_2. The mean observed O_3 concentrations for the first and second periods are 65.6 ppb and 50.4 ppb respectively; such a difference is not evident in any of the other Med-Oceanor campaigns.

The metrics reported in Table 3, refer to the first eleven days of the campaign, for the second period (in the Em_hi scenario) the mean bias is −9.27 ppb, the correlation coefficient (R) is −0.25 and the RMSE is 26.9 ppb which clearly highlights the discrepancy between the model and the observations.

The results for the spring 2004 campaign are noticeably poorer than the campaigns which took place during the summer. The model underestimates the spring 2004 O_3 concentrations by 15 ppb throughout the modelling period. The results for this year show a much higher systematic component of the RMSE as can be seen from the low value of UF-RMSE. The reasons for this are not entirely clear but are likely to be related to the spring O_3 maximum, which seems, quoting Cristofanelli and Bonasoni

ACPD
12, 16557–16602, 2012

(2009), "mainly related (Monks, 2000; Vingarzan, 2004) to stratosphere-to-troposphere exchanges (STE) and long-range transport of O_3 precursors accumulating during winter in the Northern Hemispheric free troposphere, and its ensuing in-situ photochemical production. In the free troposphere, the presence of the yearly O_3 double peak, frequently integrated in a broad spring–summer peak, is particularly evident for measurements carried out in high mountain areas."

The observations obtained during the 2006 campaign also proved difficult to reproduce. The model reproduction of the atmospheric pressure field was noticeably poorer for this campaign than for the other campaigns, and the averaged measured wind speed (and its standard deviation) were the highest of all the campaigns. Particularly during the first week of the campaign the atmospheric pressure was overestimated by the model. Using the nudging option improved both the comparison with meteorological data and with the ozone observations. For the meteorological parameters the correlation coefficient (R) improved to over 0.6, and for the ozone concentrations passed from 0.24 to 0.67. The fact that none of the other modelled periods showed much improvement with the use of nudging indicates how remarkably stable and constant meteorological conditions often are during the summer anticyclone.

The comparison between the modelled O_3 concentrations and those measured at the EMEP stations, which were within the area bounded by the finest resolution modelling domain, for each year is shown in Table 4. The results obtained are similar to those obtained for the comparison with the measurements from on-board the R. V. Urania. The most obvious difference between the results for land-based measurements and those obtained over the Mediterranean Sea, is that the model tends to overestimate the O_3 concentrations over land, with the exception of the simulations performed for the spring of 2004.

The comparison between the modelled and measured O_3 concentrations also reveals that the model does not reproduce well the amplitude of the day–night variation in concentration. This is very possibly to due to difficulties in accurately modelling the temporal evolution of the boundary layer. If the nighttime boundary layer is too high in

ACPD
12, 16557–16602, 2012

the model both the rate at which O_3 is deposited, and the rate at which it is titrated by species emitted at the surface would be underestimated. The daytime underestimate of the O_3 maximum may also be ascribed to the model's failure to correctly represent boundary layer dynamics as the mixing down of O_3 rich air plays an important role in the increase of the daytime O_3 concentration.

4.2 The influence of ship emission height in the model

As described in Sect. 3.2 two scenarios for the height at which ship emissions are introduced into the model have been studied. The first, Em_low, simply introduces all the ship emissions into the first model layer, while the second, Em_hi, distributes them between the second, third and fourth model layer, that is between 30 and 250 m, to examine the potential differences caused by plume rise (see Sect. 3.2). The results in Tables 3 and 4 show that the comparison between the measured and modelled O_3 concentrations in both instances is very similar. The emission height does have an influence on the boundary layer as a whole however; Table 5 shows the concentration differences for a number of chemical species both in the first model layer, and in the first six model layers over the marine part of the domain for the years 2005 and 2009. The top of the fifth model layer for the grid cells over the sea is close to 400 m and roughly coincides with the height of the MBL during summer anticyclonic conditions, the sixth model layer is at approximately 600 m over the Mediterranean and therefore certainly includes the whole of the MBL over the most part of the sea. The 2005 domain is more influenced by land based emissions because the cruise route was for the most part in the Adriatic Sea, the 2009 9 km by 9 km domain is significantly larger and has a higher percentage of open sea as can be seen from the route maps in Fig. 1. The differences between the ozone concentrations for the two scenarios over the whole of the simulation periods are not very large, as seen in the comparisons between the simulations and measurements in Tables 3 and 4. The difference in the averaged O_3 concentrations for the two emissions scenarios does not exceed 5 % either in the first model layer or in layers 1–6 during any of the periods simulated. This can also be seen

ACPD
12, 16557–16602, 2012

when the simulations with and without ship emissions are compared (Sect. 4.3), where the influence of the height of the emissions does not significantly alter the magnitude of the difference between the Tot_Emiss and No_ships simulations.

However looking at at the O_3 concentration field at a given time can show up significant short term differences in the simulations, as can be seen in Fig. 3. Figure 3 shows the modelled O_3 concentration and the wind arrows in the lowest model layer at midday on the 16 June 2009. The impact of the emission height on the O_3 concentrations is clear, as is the interaction between emission height and wind speed. In the Ionian Sea where the wind speed is low, emissions in the first layer influence the local O_3 more than emissions above the first layer. The same effect can be seen between Sardinia and the North African coast. However where wind speeds are higher the effect of emissions in higher model layers has a more widespread effect than emissions in the first model layer, as can be seen immediately to the west of Sardinia, where the yellow/orange area spreading northwards from the western tip of Sicily is greater in extent for the Em_hi simulation.

4.3 The influence of ship emissions

An emission inventory was prepared in which all the SNAP sector 8 (other mobile sources and machinery) emissions which occurred over the sea were removed from the database. The simulations described previously were rerun, on exactly the same domain and for exactly the same period, so that the impact of the ship emissions on the simulated concentrations, particularly of O_3 but also of other trace gases could be assessed. The simulations with all emissions have been denoted Tot_Emiss, and those without the contribution from shipping, No_ships. An overview of the results is presented in Table 6 where the difference (in %) between the concentrations of O_3, NO and NO_2 for simulations with and without shipping emissions are given. The table includes the results for both Tot_Emiss emission scenarios, Em_low and Em_hi. Roughly speaking removing the emissions from ships results in a decrease in the modelled average O_3 concentration over the whole domain by 5 or 6 ppb, and by 8 or 9 ppb over

ACPD
12, 16557–16602, 2012

the Mediterranean Sea itself, over the whole of the simulation periods. These values are significant given the size of the domain and the length of time involved, however the effect of shipping emissions is clearly not uniform over the whole domain. While Table 6 gives the average differences over the whole domain (and just the maritime part of the domain), Fig. 4 shows the time averaged impact of shipping emissions for the 2005 simulation. Figure 4 shows the difference in the average O_3 concentration in ppb in the first column, the time averaged O_3 concentration in the second column, and the difference in % in the third. The results for the Em_low emission scenario are shown in the top row and those from Em_hi in the bottom row. Not unexpectedly the greatest impact is clearly over the sea in the shipping routes where the maritime traffic is most intense. The same comparison is presented for the 2006 simulation period in Fig. 5. This campaign covered a significantly wider area and Fig. 5 shows clearly the impact on the modelled O_3 concentration along the shipping lane between the Strait of Sicily towards the entrance to the Suez Canal. Figures 4 and 5 also suggest that the impact on O_3 concentrations in coastal areas can be 10 ppb or more.

The vertical profile of the impact of ship emissions on the O_3 concentration is illustrated in Figs. 6 and 7 for the two emission scenarios. The figures show the difference in O_3 concentrations for the two latitudinal sections indicated in Fig. 2. The Med-Oceanor 2003 campaign was chosen to illustrate these profiles because it was the most wide-ranging of the cruise routes. Figure 6 shows the vertical profile of O_3 concentration (middle column) and the differences in (O_3) in ppb (first column) and % (third column), between the Tot_Emiss and No_ships scenarios. The first row is the Em_low emission scenario and the second is the Em_hi scenario. The section is not latitudinal but rather follows model cell boundaries in the Lambert-Conformal projection. In Fig. 6 the section passes through Southern Spain, crosses the coast between Valencia and Alicante, then passes across Corsica (≈10° E), then Northern Calabria in Italy, Greece and to the Eastern side Turkey. The contribution to O_3 concentrations is clearly seen to be highest in the Balearic Sea, in fact Valencia is one of the major ports in the Mediterranean. However there is also a significant contribution also in the

ACPD
12, 16557–16602, 2012

Thyrrenian and Ionian Seas. Although the absolute concentrations in the Aegean Sea, (between ≈22°and 27° E along this section), are high, the contribution to these concentrations from shipping appears to be low. This is possibly due to the relatively high emissions from other sources in the region, both Athens and Istanbul being nearby. The more southerly cross-section shown in Fig. 7 begins in Northern Morocco and meets the Mediterranean on the Gulf of Hammamet in Northern Tunisia and then crosses the southern part of the Strait of Sicily and the southernmost part of the Ionian before passing directly across Crete. At ≈15° E both the absolute O_3 and the contribution from shipping are high. This is the southern entrance to the Strait of Sicily. Again it can be seen that although absolute values are high to the eastern end of the cross-section (off the western coast of Crete) the contribution from shipping is less than in other areas. In this case this may well be because the major shipping lanes (toward Suez) are to the south of Crete and boundary layer flow during summer anticyclone conditions tends to be from north to south (Lelieveld et al., 2002). The noticeable O_3 differences over North Africa from roughly −5° to 1° E are due to the morphology of the North African coastline near the Moroccan-Algerian border. Where the Rif in North-East Morocco and the Middle (Morocco) and Tell (Algeria) Atlas mountain ranges converge there is a lower lying area, which allows the intense ship emissions in the Alboran Sea (the Mediterranean approach to the Gibraltar Strait), to make their way inland and influence O_3 concentrations by more than 10 % over 250 km inland. The effect even extends behind the Tell Atlas which would appear to be a natural barrier. Large areas of the low-lying parts of the western coast of Tunisia are affected by ship emissions (in this case from the Strait of Sicily), the average O_3 concentration increases by 5 to 10 ppb in these areas, which is 10–20 % of the total concentration. Where these increases in O_3 concentrations which result from ship emissions occur over land the vertical scale of the impact is far greater than over the sea, as can be seen in Fig. 7 over Morocco, Algeria and Tunisia. This suggests that ship emissions could contribute to the O_3 budget above the boundary layer, where due its role as a short-lived climate forcer it may have an impact on the regional radiation budget. To assess this possibility is beyond the scope of this

ACPD
12, 16557–16602, 2012

paper but given that ship emissions also include black carbon, an investigation into the potential impact of ship emissions on on regional climate may well be merited.

As mentioned above the differences in the modelled O_3 concentration with and without shipping emissions discussed so far are averaged over the whole of the campaign periods. It would be inappropriate to read too much into the difference in hourly O_3 concentrations which reach values of as much as 40–50 ppb in certain areas, but to gain an insight into how serious the contribution to local ozone levels ship emissions might be, the eight-hour average O_3 concentraion has been investigated. The current air quality standard for O_3 in the European Union is a maximum daily 8 h mean of 120 $\mu g\,m^{-3}$ which given the summer temperatures during the oceanographic campaigns is between 60 and 62 ppb. The model output has been investigated to determine how often the difference between the Tot_Emiss and No_ships simulations is such that contribution from ships tips the scales between complying to the EU air quality standard and not complying. Examples of the results obtained are shown in Figs. 8 and 9 for one Em_low and one Em_hi scenario. For the year 2005 the model suggests that some areas of the Italian coast that ship emissions contributed to local ozone concentrations to such an extent that for 50 % of the days of the simulation period the EU air quality standard exceedance would have been avoided had there been no ship emissions.

5 Conclusions

The WRF/Chem model has been used to simulate O_3 concentrations for the periods of seven oceanographic research campaigns which took place in the Mediterranean Basin between 2000 and 2010. The results of the comparison between the model and observations are quantitatively similar to results obtained in previous studies using the WRF model. The results for the wind speed were not as good as previous studies, however the prevailing anticyclonic conditions during all but one of the simulation periods resulted in low wind speeds which are known to be difficult to reproduce. The results of the comparison between the modelled O_3 concentration with the exception of the

ACPD
12, 16557–16602, 2012

spring 2004 campaign showed a reasonable agreement. The mean bias between measurements and the model was lower for shipboard measurements than for observations from the land based EMEP sites, while the correlation between the model and the measurements was higher for the EMEP sites. The model has some problems reproducing the variation between the day time maxima and the night-time minima at some of the EMEP sites, although the timing of the daily cycle, as reflected by the correlation coefficient, was reproduced well. It is possible that the lower correlation between the model and shipboard measurements was in part due to the sporadic interception of relatively fresh ship plumes which caused atypical fluctuations in the O_3 concentrations. Certainly during the 2003 cruise campaign which arrived almost at the Strait of Gibraltar there was a noticeable effect on O_3 close to the major shipping lanes in the Alboran Sea. Simulations were performed to investigate the influence of emission height for ship plumes on the production and distribution of O_3. These simulations indicate that long-term average O_3 concentrations in the region are not greatly influenced by the way the ship emissions are distributed throughout the lowest model layers. However in the short-term the local impact can be very different depending on the assumptions made concerning the effective release height of ship emissions. If the emissions are assumed to be released above the lowest model layer their impact can be far more widespread than if they are assumed to be admitted into the lowest model layer (≈30 m in these simulations), however this is most noticeable comparing specific times. The effect of the height of the emissions is far less obvious when an 8 or 24 h average is considered. When comparing the difference between simulations with and without ship emissions, the height of the ship emissions really makes very little difference because the overriding factor is their presence rather than their whereabouts. At any given time near the shipping lanes the difference in the O_3 concentration between the simulations with and without ship emissions can be greater than 40 ppb, more generally over the periods simulated here the difference in the average O_3 concentration was 10 to 20 % over the MBL, and 5 to 15 % over the whole of the highest resolution modelling domain. Given that the average measured O_3 concentrations during the Med-Oceanor

ACPD
12, 16557–16602, 2012

series of oceanographic measurement campaigns was 50–60 ppb, shipping emissions can contribute between ≈3 and 12 ppb to the long-term average concentrations of O_3. The influence of the ship emissions on O_3 levels is mostly constrained to coastal areas as a result of the low summer time Mediterranean MBL height and the steepness of much of the Mediterranean coastline. However as the investigation of the vertical profiles of O_3 illustrated some areas, particularly the flatter coastal areas in North Africa showed a significant impact on O_3 from shipping emissions tens and even hundreds of km inland. As the ship emissions can influence O_3 some distance inland it is possible that their impact will also be noticeable above the boundary layer, especially if the anticyclonic conditions typical of summertime Mediterranean weather persist. To establish whether this is case is beyond the scope of this study, but would merit further investigation with longer term simulations. The extent to which shipping emissions can affect air quality is made clear by the sizeable area of the modelling domains which would not exceed the EU 8 h average concentration of 120 $\mu g\,m^{-3}$ in the simulations where they are not included. As maritime traffic is projected to increase in the coming years, and as legislation leads to diminishing emissions from land based sources, the relative contribution of shipping to total O_3 precursor emissions will increase. Shipping emissions will therefore continue to play an important role in local and regional air quality in Mediterranean coastal areas and beyond for the foreseeable future.

Acknowledgements. The meteorological input data used in this study are from the Research Data Archive (RDA) which is maintained by the Computational and Information Systems Laboratory (CISL) at the National Center for Atmospheric Research (NCAR). NCAR is sponsored by the National Science Foundation (NSF). The original data are available from the RDA (http://dss.ucar.edu) in dataset number ds083.2. The authors gratefully acknowledge the financial support received from the GMOS project (European Commission Seventh Framework Programme ENV.2010.4.1.3-2 Global Observation Systems for Mercury, http://www.gmos.eu/)

ACPD
12, 16557–16602, 2012

References

Adame, J. A., Serrano, E., Bolívar, J. P., and de la Morena, B. A.: On the tropospheric ozone variations in a coastal area of Southwestern Europe under a mesoscale circulation, J. Appl. Meteor. Climatol., 49, 748–759, 2009.

Andersson, M. E., Gårdfeldt, K., Wängberg, I., Sprovieri, F., Pirrone, N., and Lindqvist, O.: Reprint of "Seasonal and daily variation of mercury evasion at coastal and off shore sites from the Mediterranean Sea", Mar. Chem., 107, 104–116, 2007.

Auvray, M. and Bey, I.: Long-range transport to Europe: seasonal variations and implications for the European ozone budget, J. Geophys. Res., 110, D11303, 2005.

Bonasoni, P., Stohl, A., Cristofanelli, P., Calzolari, F., Colombo, T., and Evangelisti, F.: Background ozone variations at Mt. Cimone Station, Atmos. Environ., 34, 5183–5189, 2000.

Capaldo, K., Corbett, J. J., Kasibhatla, P., Fischbeck, P., and Pandis, S. N.: Effects of ship emissions on sulphur cycling and radiative climate forcing over the ocean, Nature, 400, 743–746, 1999.

Chang, J. C. and Hanna, S. R.: Air quality model performance evaluation, Meteorol. Atmos. Phys., 87, 167–196, 2004.

Charlton-Perez, C. L., Evans, M. J., Marsham, J. H., and Esler, J. G.: The impact of resolution on ship plume simulations with NO_x chemistry, Atmos. Chem. Phys., 9, 7505–7518, doi:10.5194/acp-9-7505-2009, 2009.

Chosson, F., Paoli, R., and Cuenot, B.: Ship plume dispersion rates in convective boundary layers for chemistry models, Atmos. Chem. Phys., 8, 4841–4853, doi:10.5194/acp-8-4841-2008, 2008.

Corbett, J. J., Winebrake, J. J., Green, E. H., Kasibhatla, P., Eyring, V., and Lauer, A.: Mortality from ship emissions: a global assessment, Environ. Sci. Technol., 41, 8512–8518, 2007.

Cristofanelli, P. and Bonasoni, P.: Background ozone in the Southern Europe and Mediterranean Area: influence of the transport processes, Environ. Pollut., 157, 1399–1406, 2009.

Cristofanelli, P., Bonasoni, P., Carboni, G., Calzolari, F., Casarola, L., Sajani, S. Z., and Santaguida, R.: Anomalous high ozone concentrations recorded at a high mountain station in Italy in summer 2003, Atmos. Environ., 41, 1383–1394, 2007.

Dalsøren, S. B., Eide, M. S., Endresen, Ø., Mjelde, A., Gravir, G., and Isaksen, I. S. A.: Update on emissions and environmental impacts from the international fleet of ships: the contribution

ACPD
12, 16557–16602, 2012

from major ship types and ports, Atmos. Chem. Phys., 9, 2171–2194, doi:10.5194/acp-9-2171-2009, 2009.
de Meij, A., Gzella, A., Cuvelier, C., Thunis, P., Bessagnet, B., Vinuesa, J. F., Menut, L., and Kelder, H. M.: The impact of MM5 and WRF meteorology over complex terrain on CHIMERE model calculations, Atmos. Chem. Phys., 9, 6611–6632, doi:10.5194/acp-9-6611-2009, 2009.
Derwent, R. G., Stevenson, D. S., Doherty, R. M., Collins, W. J., Sanderson, M. G., Johnson, C. E., Cofala, J., Mechler, R., Amann, M., and Dentener, F. J.: The contribution from shipping emissions to air quality and acid deposition in Europe, AMBIO, 34, 54–59, 2005.
Duncan, B. N., West, J. J., Yoshida, Y., Fiore, A. M., and Ziemke, J. R.: The influence of European pollution on ozone in the Near East and northern Africa, Atmos. Chem. Phys., 8, 2267-2283, doi:10.5194/acp-8-2267-2008, 2008.
Eyring, V., Köhler, H. W., van Aardenne, J., and Lauer, A.: Emissions from international shipping: 1. the last 50 years, J. Geophys. Res., 110, D17305, doi:10.1029/2004JD005619, 2005.
Eyring, V., Stevenson, D. S., Lauer, A., Dentener, F. J., Butler, T., Collins, W. J., Ellingsen, K., Gauss, M., Hauglustaine, D. A., Isaksen, I. S. A., Lawrence, M. G., Richter, A., Rodriguez, J. M., Sanderson, M., Strahan, S. E., Sudo, K., Szopa, S., van Noije, T. P. C., and Wild, O.: Multi-model simulations of the impact of international shipping on Atmospheric Chemistry and Climate in 2000 and 2030, Atmos. Chem. Phys., 7, 757–780, doi:10.5194/acp-7-757-2007, 2007.
Eyring, V., Isaksen, I. S., Berntsen, T., Collins, W. J., Corbett, J. J., Endresen, Ø., Grainger, R. G., Moldanova, J., Schlager, H., and Stevenson, D. S.: Transport impacts on atmosphere and climate: shipping, Atmos. Environ., 44, 4735–4771, 2010.
Fast, J. D., Gustafson, William I., J., Easter, R. C., Zaveri, R. A., Barnard, J. C., Chapman, E. G., Grell, G. A., and Peckham, S. E.: Evolution of ozone, particulates, and aerosol direct radiative forcing in the vicinity of Houston using a fully coupled meteorology-chemistry-aerosol model, J. Geophys. Res., 111, D21305, 2006.
Ferrara, R., Ceccarini, C., Lanzillotta, E., Gårdfeldt, K., Sommar, J., Horvat, M., Logar, M., Fajon, V., and Kotnik, J.: Profiles of dissolved gaseous mercury concentration in the Mediterranean seawater, Atmos. Environ., 37, 85–92, 2003.
Gårdfeldt, K., Sommar, J., Ferrara, R., Ceccarini, C., Lanzillotta, E., Munthe, J., Wängberg, I., Lindqvist, O., Pirrone, N., Sprovieri, F., Pesenti, E., and Strömberg, D.: Evasion of mercury

ACPD
12, 16557–16602, 2012

from coastal and open waters of the Atlantic Ocean and the Mediterranean Sea, Atmos. Environ., 37, 73–84, 2003.
Geng, F., Zhao, C., Tang, X., Lu, G., and Tie, X.: Analysis of ozone and VOCs measured in Shanghai: a case study, Atmos. Environ., 41, 989–1001, 2007.
Gerasopoulos, E., Kouvarakis, G., Vrekoussis, M., Kanakidou, M., and Mihalopoulos, N.: Ozone variability in the marine boundary layer of the Eastern Mediterranean based on 7-year observations, J. Geophys. Res., 110, D15309, 2005.
Grell, G. A., Peckham, S. E., Schmitz, R., McKeen, S. A., Frost, G., Skamarock, W. C., and Eder, B.: Fully coupled "online" chemistry within the WRF model, Atmos. Environ., 39, 6957–6975, 2005.
Guenther, A., Zimmerman, P., and Wildermuth, M.: Natural volatile organic compound emission rate estimates for US woodland landscapes, Atmos. Environ., 28, 1197–1210, 1994.
Guenther, A. B., Zimmerman, P. R., Harley, P. C., Monson, R. K., and Fall, R.: Isoprene and monoterpene emission rate variability: model evaluations and sensitivity analyses, J. Geophys. Res., 98, 12609–12617, 1993.
Hjellbrekke, A.-G., Solberg, S., and Fjæraa, A. M.: Ozone measurements 2009, EMEP/CCC-Report 2/2011, Tech. rep., EMEP (European Monitoring and Evaluation Programme), reports on measurement data for all years are available at: http://www.nilu.no/projects/ccc/reports.html, 2011.
Hu, X. and Zhang, Y.: Implementation and testing of a new aerosol module in WRF/Chem, in: 14th Joint Conference on the Applications of Air Pollution Meteorology with the Air and Waste Management Assoc, 2006.
Huszar, P., Cariolle, D., Paoli, R., Halenka, T., Belda, M., Schlager, H., Miksovsky, J., and Pisoft, P.: Modeling the regional impact of ship emissions on NO_x and ozone levels over the Eastern Atlantic and Western Europe using ship plume parameterization, Atmos. Chem. Phys., 10, 6645–6660, doi:10.5194/acp-10-6645-2010, 2010.
Im, U. and Kanakidou, M.: Summertime impacts of Eastern Mediterranean megacity emissions on air quality, Atmos. Chem. Phys. Discuss., 11, 26657–26690, doi:10.5194/acpd-11-26657-2011, 2011.
IPCC: Climate Change 2007: The Physical Science Basis, the Fourth Assessment Report of the IPCC, Tech. rep., Intergovernmental Panel on Climate Change (IPCC), 2007.
Kalabokas, P. D., Volz-Thomas, A., Brioude, J., Thouret, V., Cammas, J.-P., and Repapis, C. C.: Vertical ozone measurements in the troposphere over the Eastern Mediterranean and

ACPD
12, 16557–16602, 2012

comparison with Central Europe, Atmos. Chem. Phys., 7, 3783–3790, doi:10.5194/acp-7-3783-2007, 2007.
Kalabokas, P., Mihalopoulos, N., Ellul, R., Kleanthous, S., and Repapis, C.: An investigation of the meteorological and photochemical factors influencing the background rural and marine surface ozone levels in the Central and Eastern Mediterranean, Atmos. Environ., 42, 7894–7906, 2008.
Kanakidou, M., Mihalopoulos, N., Kindap, T., Im, U., Vrekoussis, M., Gerasopoulos, E., Dermitzaki, E., Unal, A., Koçak, M., Markakis, K., Melas, D., Kouvarakis, G., Youssef, A. F., Richter, A., Hatzianastassiou, N., Hilboll, A., Ebojie, F., Wittrock, F., von Savigny, C., Burrows, J. P., Ladstaetter-Weissenmayer, A., and Moubasher, H.: Megacities as hot spots of air pollution in the East Mediterranean, Atmos. Environ., 45, 1223–1235, 2011.
Kotnik, J., Horvat, M., Tessier, E., Ogrinc, N., Monperrus, M., Amouroux, D., Fajon, V., Gibičar, D., Žižek, S., Sprovieri, F., and Pirrone, N.: Mercury speciation in surface and deep waters of the Mediterranean Sea, Mar. Chem., 107, 13–30, 2007.
Lawrence, M. G. and Crutzen, P. J.: Influence of NO_x emissions from ships on tropospheric photochemistry and climate, Nature, 402, 167–170, 1999.
Lelieveld, J., Berresheim, H., Borrmann, S., Crutzen, P. J., Dentener, F. J., Fischer, H., Feichter, J., Flatau, P. J., Heland, J., Holzinger, R., Korrmann, R., Lawrence, M. G., Levin, Z., Markowicz, K. M., Mihalopoulos, N., Minikin, A., Ramanathan, V., de Reus, M., Roelofs, G. J., Scheeren, H. A., Sciare, J., Schlager, H., Schultz, M., Siegmund, P., Steil, B., Stephanou, E. G., Stier, P., Traub, M., Warneke, C., Williams, J., and Ziereis, H.: Global air pollution crossroads over the Mediterranean, Science, 298, 794–799, 2002.
Lowe, P. R.: An approximating polynomial for the computation of saturation vapor pressure, J. Appl. Meteorol., 16, 100–103, 1977.
Madronich, S.: Photodissociation in the atmosphere. 1. Actinic flux and the effects of ground reflections and clouds, J. Geophys. Res., 92, 9740–9752, 1987.
Marmer, E. and Langmann, B.: Impact of ship emissions on the Mediterranean summertime pollution and climate: a regional model study, Atmos. Environ., 39, 4659–4669, 2005.
Marmer, E., Dentener, F., Aardenne, J. v., Cavalli, F., Vignati, E., Velchev, K., Hjorth, J., Boersma, F., Vinken, G., Mihalopoulos, N., and Raes, F.: What can we learn about ship emission inventories from measurements of air pollutants over the Mediterranean Sea?, Atmos. Chem. Phys., 9, 6815–6831, doi:10.5194/acp-9-6815-2009, 2009.

ACPD
12, 16557–16602, 2012

Matthias, V., Bewersdorff, I., Aulinger, A., and Quante, M.: The contribution of ship emissions to air pollution in the North Sea regions, Environ. Pollut., 158, 2241–2250, 2010.
Millán, M. M., Sanz, M. J., Salvador, R., and Mantilla, E.: Atmospheric dynamics and ozone cycles related to nitrogen deposition in the Western Mediterranean, Environ. Pollut., 118, 167–186, 2002.
Miola, A. and Ciuffo, B.: Estimating air emissions from ships: meta-analysis of modelling approaches and available data sources, Atmos. Environ., 45, 2242–2251, 2011.
Misenis, C. and Zhang, Y.: An examination of sensitivity of WRF/Chem predictions to physical parameterizations, horizontal grid spacing, and nesting options, Atmos. Res., 97, 315–334, 2010.
Monks, P. S.: A review of the observations and origins of the spring ozone maximum, Atmos. Environ., 34, 3545–3561, 2000.
Monks, P. S., Granier, C., Fuzzi, S., Stohl, A., Williams, M., Akimoto, H., Amann, M., Baklanov, A., Baltensperger, U., Bey, I., Blake, N., Blake, R., Carslaw, K., Cooper, O., Dentener, F., Fowler, D., Fragkou, E., Frost, G., Generoso, S., Ginoux, P., Grewe, V., Guenther, A., Hansson, H., Henne, S., Hjorth, J., Hofzumahaus, A., Huntrieser, H., Isaksen, I., Jenkin, M., Kaiser, J., Kanakidou, M., Klimont, Z., Kulmala, M., Laj, P., Lawrence, M., Lee, J., Liousse, C., Maione, M., McFiggans, G., Metzger, A., Mieville, A., Moussiopoulos, N., Orlando, J., O'Dowd, C., Palmer, P., Parrish, D., Petzold, A., Platt, U., Pöschl, U., Prévôt, A., Reeves, C., Reimann, S., Rudich, Y., Sellegri, K., Steinbrecher, R., Simpson, D., ten Brink, H., Theloke, J., van der Werf, G., Vautard, R., Vestreng, V., Vlachokostas, C., and von Glasow, R.: Atmospheric composition change – global and regional air quality, Atmos. Environ., 43, 5268–5350, 2009.
Nolle, M., Ellul, R., Heinrich, G., and Güsten, H.: A long-term study of background ozone concentrations in the Central Mediterranean – diurnal and seasonal variations on the island of Gozo, Atmos. Environ., 36, 1391–1402, 2002.
Saliba, M., Ellul, R., Camilleri, L., and Güsten, H.: A 10-year study of background surface ozone concentrations on the island of Gozo in the Central Mediterranean, J. Atmos. Chem., 60, 117–135, doi:10.1007/s10874-008-9112-3, 2008.
Schürmann, G. J., Algieri, A., Hedgecock, I. M., Manna, G., Pirrone, N., and Sprovieri, F.: Modelling local and synoptic scale influences on ozone concentrations in a topographically complex region of Southern Italy, Atmos. Environ., 43, 4424–4434, 2009.

ACPD
12, 16557–16602, 2012

Simpson, D., Guenther, A., Hewitt, C. N., and Steinbrecher, R.: Biogenic emissions in Europe. 1. Estimates and uncertainties, J. Geophys. Res., 100, 22875–22890, 1995.
Simpson, D., Fagerli, H., Jonson, J., Tsyro, S., Wind, P., and Tuovinen, J.: Trans-boundary acidication and eutrophication and ground level ozone in Europe: Unified EMEP model description, EMEP Status Report 1/2003 Part I, EMEP/MSC-W Report, The Norwegian Meteorological Institute, Oslo, Norway, 2003.
Skamarock, W. C., Klemp, J. B., Dudhia, J., Gill, D. O., Barker, D. M., Duda, M. G., Huang, X.-Y. Wang, W., and Powers, J. G.: A Description of the Advanced Research WRF Version 3, Tech. rep., National Center for Atmospheric Research, 2008.
Song, C. H., Chen, G., Hanna, S. R., Crawford, J., and Davis, D. D.: Dispersion and chemical evolution of ship plumes in the marine boundary layer: investigation of $O_3/NO_y/HO_x$ chemistry, J. Geophys. Res., 108, 4143, 2003.
Song, S.-K., Shon, Z.-H., Kim, Y.-K., Kang, Y.-H., Oh, I.-B., and Jung, C.-H.: Influence of ship emissions on ozone concentrations around coastal areas during summer season, Atmos. Environ., 44, 713–723, 2010.
Sprovieri, F., Pirrone, N., Gårdfeldt, K., and Sommar, J.: Mercury speciation in the marine boundary layer along a 6000 km cruise path around the Mediterranean Sea, Atmos. Environ., 37, 63–71, 2003.
Sprovieri, F., Hedgecock, I. M., and Pirrone, N.: An investigation of the origins of reactive gaseous mercury in the Mediterranean marine boundary layer, Atmos. Chem. Phys., 10, 3985–3997, doi:10.5194/acp-10-3985-2010, 2010.
Stockwell, W. R., Middleton, P., Chang, J. S., and Taang, X.: The second-generation regional acid deposition model chemical mechanism for regional air quality modelling, J. Geophys. Res., 95, 16343–16367, 1990.
Tie, X., Madronich, S., Li, G. H., Ying, Z., Zhang, R., Garcia, A., Lee-Taylor, J., and Liu, Y.: Characterizations of chemical oxidants in Mexico City: a regional chemical dynamical model (WRF-Chem) study, Atmos. Environ., 41, 1989–2008, 2007.
Tuccella, P., Curci, G., Visconti, G., Bessagnet, B., Menut, L., and Park, R. J.: Modeling of gas and aerosol with WRF/Chem over Europe: evaluation and sensitivity study, J. Geophys. Res., 117, D03303, 2012.
Velchev, K., Cavalli, F., Hjorth, J., Marmer, E., Vignati, E., Dentener, F., and Raes, F.: Ozone over the Western Mediterranean Sea – results from two years of shipborne measurements, Atmos. Chem. Phys., 11, 675–688, doi:10.5194/acp-11-675-2011, 2011.

ACPD
12, 16557–16602, 2012

Vestreng, V., Mareckova, K., Kakareka, S., Malchykhina, A., and Kukharchyk, T.: Inventory Review 2007; Emission Data reported to LRTAP Convention and NEC Directive, MSC-W Technical Report 1/07,, Tech. rep., The Norwegian Meteorological Institute, Oslo, Norway, 2007.
Vingarzan, R.: A review of surface ozone background levels and trends, Atmos. Environ., 38, 3431–3442, 2004.
Vinken, G. C. M., Boersma, K. F., Jacob, D. J., and Meijer, E. W.: Accounting for non-linear chemistry of ship plumes in the GEOS-Chem global chemistry transport model, Atmos. Chem. Phys., 11, 11707–11722, doi:10.5194/acp-11-11707-2011, 2011.
von Glasow, R., Lawrence, M. G., Sander, R., and Crutzen, P. J.: Modeling the chemical effects of ship exhaust in the cloud-free marine boundary layer, Atmos. Chem. Phys., 3, 233–250, doi:10.5194/acp-3-233-2003, 2003.
Vutukuru, S. and Dabdub, D.: Modeling the effects of ship emissions on coastal air quality: a case study of Southern California, Atmos. Environ., 42, 3751–3764, 2008.
Wallace, J. M. and Hobbs, P. V.: Atmospheric Science: An Introductory Survey, Academic Press, New York, 1977.
Willmott, C. J., Davis, R. E., Feddema, J. J., Klink, K. M., Legates, D. R., Rowe, C. M., Ackleson, S. G., and O'Donnell, J.: Statistics for the evaluation and comparison of models, J. Geophys. Res, 90, 8995–9005, 1985.
Worden, H. M., Bowman, K. W., Kulawik, S. S., and Aghedo, A. M.: Sensitivity of outgoing longwave radiative flux to the global vertical distribution of ozone characterized by instantaneous radiative kernels from Aura-TES, J. Geophys. Res., 116, D14115, 2011.
Zhang, Y.: Online-coupled meteorology and chemistry models: history, current status, and outlook, Atmos. Chem. Phys., 8, 2895–2932, doi:10.5194/acp-8-2895-2008, 2008.
Zhang, Y. and Dubey, M. K.: Comparisons of WRF/Chem simulated O_3 concentrations in Mexico City with ground-based RAMA measurements during the MILAGRO period, Atmos. Environ., 43, 4622–4631, 2009.

ACPD
12, 16557–16602, 2012

Table 1. The metrics used to assess the model performance.

Metric	Definition
Mean bias	$\mathrm{MB} = \overline{X}_{\mathrm{obs}} - \overline{X}_{\mathrm{mod}}$
Correlation coefficient	$\mathrm{R} = \frac{\left(X_{\mathrm{obs}} - \overline{X}_{\mathrm{obs}}\right)\left(X_{\mathrm{mod}} - \overline{X}_{\mathrm{mod}}\right)}{\sigma_{\mathrm{obs}}\sigma_{\mathrm{mod}}}$
Root mean square error	$\mathrm{RMSE} = \sqrt{\left(\overline{X}_{\mathrm{obs}} - X_{\mathrm{obs}}\right)^2}$
Unsystematic fraction of RMSE	$\mathrm{UF}_{\mathrm{RMSE}} = \frac{\mathrm{RMSE}_u^2}{\mathrm{RMSE}^2}$
Index of agreement	$\mathrm{IOA} = 1 - \frac{\mathrm{N} \cdot \mathrm{RMSE}^2}{\sum_{i=1}^{N}\left(\left\lvert X_{\mathrm{mod}}^{(i)} - \overline{X}_{\mathrm{mod}}\right\rvert + \left\lvert X_{\mathrm{obs}}^{(i)} - \overline{X}_{\mathrm{obs}}\right\rvert\right)^2}$

ACPD
12, 16557–16602, 2012

Table 2. Comparison between the model output and meteorological parameters measured aboard the R. V. Urania. There was no relative humidity data available for 2010.

	2000	2003	2004	2005	2006	2009	2010
				Temperature			
MB/(°C)	1.3	2.3	1.7	8.2	1.9	2.6	2.0
R	0.55	0.32	0.45	0.58	0.46	0.75	0.79
RMSE/(°C)	1.9	2.9	2.1	8.9	2.2	3.1	2.4
UF-RMSE	0.43	0.25	0.18	0.02	0.18	0.26	0.30
IOA	0.64	0.46	0.54	0.44	0.44	0.63	0.71
				Wind speed			
MB/(ms^{-1})	−0.97	0.80	1.03	0.13	1.34	−0.9	−0.32
R	0.23	0.32	0.42	0.16	0.43	0.12	0.45
RMSE/(ms^{-1})	4.2	3.3	4.3	3.8	4.3	4.7	3.5
UF-RMSE	0.55	0.63	0.55	0.63	0.45	0.62	0.75
IOA	0.54	0.60	0.65	0.50	0.65	0.44	0.69
				Relative humidity			
MB/(%)	−2.5	2.67	−10.8	9.0	−5.1	−2.4	
R	0.19	0.30	0.17	−0.01	0.23	0.34	
RMSE/(%)	15.0	14.0	16.7	18.6	14.0	14.4	
UF-RMSE	0.75	0.35	0.19	0.51	0.71	0.88	
IOA	0.5	0.56	0.47	0.32	0.50	0.57	

ACPD
12, 16557–16602, 2012

Table 3. Comparison of the model results and the ozone concentrations measured aboard the R. V. Urania, see Sect. 3.2 for the definition of the Em_low amd Em_hi emission scenarios. UF refers to the unsystematic fraction of the RMSE. The results for 2003 consider only the first half of the campaign, see Sect. 4.1.2.

	Em_low scenario					Em_hi scenario				
Year	MB (ppb)	*R*	RMSE (ppb)	UF	IOA	MB (ppb)	*R*	RMSE (ppb)	UF	IOA
2000	−3.7	0.51	11.0	0.59	0.69	0.66	0.59	9.6	0.68	0.76
2003	4.0	0.32	14.7	0.47	0.55	3.7	0.31	14.7	0.48	0.54
2004	15.1	0.02	18.5	0.07	0.39	16.1	−0.14	19.8	0.07	0.36
2005	3.0	0.55	13.8	0.80	0.73	4.57	0.56	13.5	0.69	0.72
2006	9.9	0.24	14.5	0.33	0.48	−8.8	0.19	14.3	0.40	0.49
2009	7.8	0.30	14.9	0.55	0.53	7.89	0.29	15.3	0.56	0.52
2010	−0.7	0.39	10.7	0.73	0.63	−1.2	0.38	10.9	0.73	0.63

ACPD
12, 16557–16602, 2012

Table 4. Comparison of the model results and the ozone concentrations measured at the EMEP stations within the highest resolution modelling domain, see Sect. 3.2 for the description of the Em_low and Em_hi emission scenarios. The stations are ES07 Víznar, ES10 Cabo de Creus, ES12 Zarra, ES14 Els Torms, FR13 Peyrusse Vieille, FR16 Le Casset, FR17 Montfranc, GR02 Finokalia, GR03 Livadi, IT01 Montelibretti, IT04 Ispra, MT01 Giordan Lighthouse. The locations of the EMEP stations are shown in Fig. 1. UF refers to the unsystematic fraction of the RMSE.

		Em_low scenario					Em_hi scenario				
Year	Station	MB (ppb)	*R*	RMSE (ppb)	UF	IOA	MB (ppb)	*R*	RMSE (ppb)	UF	IOA
2000	GR03	−6.1	0.53	17.1	0.84	0.68	1.0	0.53	14.2	0.87	0.72
	IT01	−12.3	0.24	30.4	0.36	0.53	−9.2	0.29	27.2	0.27	0.54
	MT01	−10.2	0.46	17.6	0.65	0.55	−9.9	0.20	19.7	0.64	0.44
2003	ES07	−5.5	0.20	15.8	0.54	0.50	−5.5	0.19	15.9	0.53	0.50
	ES12	−0.8	0.15	15.6	0.60	0.48	−1.2	0.14	15.8	0.59	0.48
	ES14	−3.8	0.26	15.1	0.39	0.52	−4.0	0.24	15.3	0.39	0.51
	GR02	−1.3	0.66	7.5	0.94	0.80	−1.4	0.66	7.6	0.93	0.79
	IT01	−13.4	0.61	24.5	0.29	0.68	−13.4	0.59	24.8	0.29	0.67
	MT01	−5.2	0.17	15.0	0.66	0.47	−5.9	0.16	15.8	0.66	0.45
2004	ES10	13.4	0.28	15.5	0.16	0.38	13.7	0.29	15.7	0.16	0.38
	ES14	5.2	0.31	11.5	0.53	0.53	5.1	0.32	11.4	0.53	0.53
	FR13	7.3	0.49	11.2	0.49	0.59	7.3	0.48	11.2	0.50	0.59
	FR16	14.6	0.59	15.6	0.04	0.44	14.5	0.58	15.5	0.04	0.44
	FR17	10.3	0.14	14.2	0.25	0.41	10.2	0.14	14.1	0.26	0.41
	IT01	−13.5	0.50	18.8	0.30	0.59	−13.9	0.52	18.9	0.27	0.59
	IT04	−6.5	0.64	13.6	0.42	0.74	−6.7	0.63	13.7	0.41	0.73
2005	IT01	−17.0	0.64	24.4	0.20	0.67	−17.1	0.64	24.4	0.20	0.67
	IT04	−25.3	0.78	29.6	0.20	0.69	−25.3	0.78	29.7	0.20	0.69
2006	IT01	−15.7	0.80	23.1	0.11	0.70	−16.2	0.80	23.3	0.10	0.70
	MT01	−16.4	0.25	22.1	0.44	0.28	−16.9	0.25	22.7	0.44	0.27
2009	IT01	−2.9	0.72	15.4	0.19	0.72	−3.0	0.72	15.4	0.19	0.72

ACPD
12, 16557–16602, 2012

Table 5. Concentration differences between the Em_low and Em_hi scenarios, over the marine part of the 9 km modelling domain (Em_low – Em_hi). (Percentage differences calculated as (Em_low – Em_hi)/Em_low × 100 %).

Year	Level	O_3 (ppb)	NO (ppt)	NO_2 (ppb)	SO_2 (ppb)	HO (molec. cm^{-3})	HCHO (ppb)	HNO_3 (ppb)
2005	Av. conc. Em_low, level 1	57.3	72.9	1.2	1.4	4.7×10^5	6.0	0.94
	difference level 1	2.7	21.1	0.38	0.29	1.1×10^5	0.65	0.11
	difference levels 1–6	−1.1	−1.3	−0.026	−0.18	-1.4×10^4	−0.21	0.08
2009	Av. conc. Em_low, level 1	48.2	66.2	0.86	0.89	8.4×10^5	2.7	0.61
	difference level 1	1.8	11.3	0.19	0.20	6.3×10^4	0.33	0.05
	difference levels 1–6	0.01	−1.5	−0.021	−0.026	-1.9×10^5	0.12	0.02
					Percentage differences			
2005	level 1	4.6	28.9	31.4	20.5	23.6	11.6	1.4
	levels 1–6	−1.7	−4.4	−6.1	−11.3	−3.8	−3.8	−6.9
2009	level 1	3.7	17.1	22.5	22.8	−7.4	12.1	8.5
	levels 1–6	0.0	−4.7	−5.8	2.6	−27.6	4.4	2.7

ACPD
12, 16557–16602, 2012

Table 6. The influence (%) of shipping emissions on the average concentrations of O_3, NO and NO_2 in the lowest model layer and on the first six layers (over the marine parts of the modelling domain). Calculated as (Tot_Emiss – No_Ships)/Tot_Emiss × 100 %.

		Whole domain						Mediterranean Sea					
		Em_low			Em_hi			Em_low			Em_hi		
Year	Level	O_3	NO	NO_2	O_3	NO	NO_2	O_3	NO	NO_2	O_3	NO	NO_2
2000	1	11.4	22.9	21.9	8.8	15.1	14.2	15.2	40.3	43.9	10.7	27.7	29.7
	1–6	4.3	10.1	10.1	5.5	11.2	11.9	4.8	18.2	20.3	6.2	20.0	23.2
2003	1	9.3	17.9	16.3	9.6	13.0	12.5	11.7	40.4	42.0	12.3	31.8	34.4
	1–6	6.5	9.8	10.2	7.0	10.3	11.0	7.5	23.7	27.2	8.2	24.9	28.9
2004	1	9.5	30.7	21.3	8.7	21.0	15.0	13.9	57.9	53.9	12.4	44.8	42.6
	1–6	5.5	16.0	13.0	5.9	1.0	14.4	9.1	45.5	44.6	9.3	43.8	43.3
2005	1	10.5	19.4	16.0	8.3	9.2	7.6	17.0	44.2	44.5	13.1	25.6	26.0
	1–6	3.6	5.7	6.1	4.5	6.9	7.4	7.5	27.7	30.3	8.2	25.0	27.7
2006	1	11.7	27.4	25.8	10.6	19.5	18.3	14.4	42.4	45.5	12.9	32.1	35.0
	1–6	4.3	11.2	11.5	5.3	12.2	13.1	7.5	27.7	31.6	8.3	26.9	30.9
2009	1	16.3	36.5	34.2	15.1	31.2	28.2	19.9	55.3	57.8	17.4	46.9	47.4
	1–6	8.3	19.1	20.1	9.1	20.2	21.8	11.8	41.1	45.2	11.6	42.6	46.0
2010	1	9.0	20.0	16.7	9.7	16.3	12.3	10.5	35.7	36.4	11.3	31.2	31.9
	1–6	7.1	15.7	14.1	7.7	15.9	13.8	9.1	30.1	32.6	9.8	30.1	32.7

ACPD
12, 16557–16602, 2012

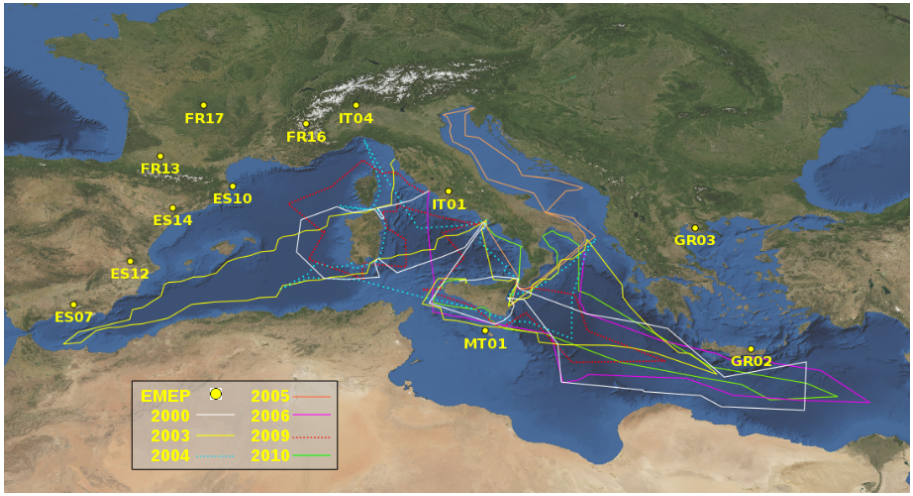

Fig. 1. The Med-Oceanor campaign routes over the years. Also shown are the sites of the EMEP stations used in the model validation.

ACPD
12, 16557–16602, 2012

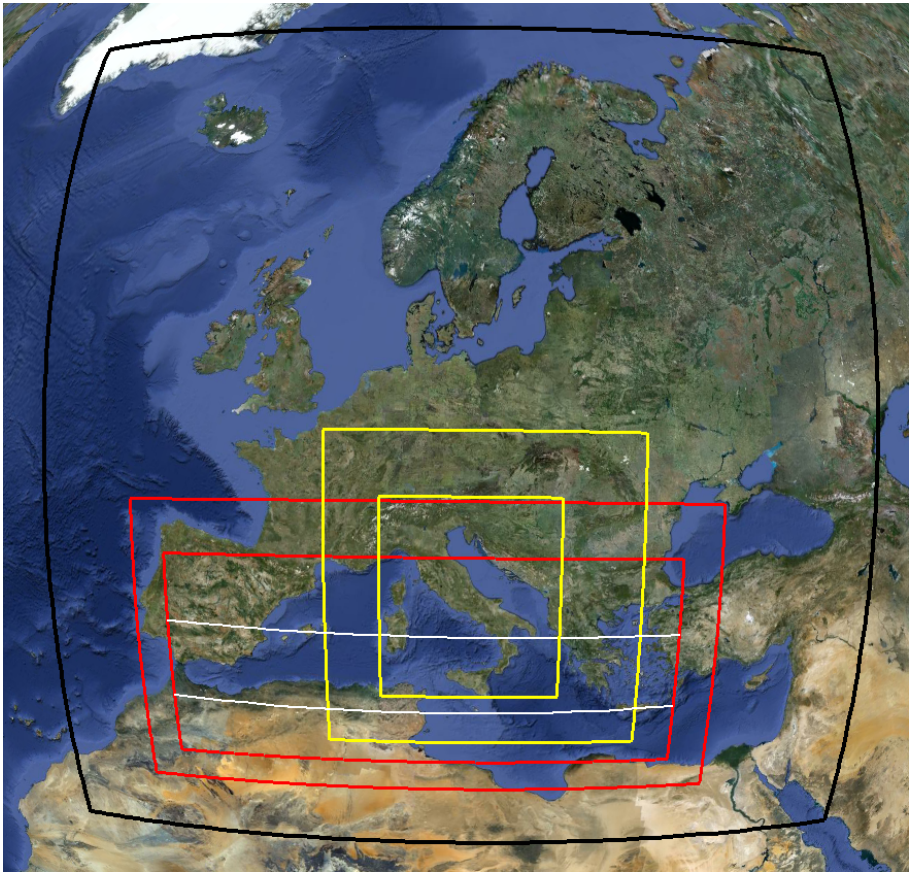

Fig. 2. The largest modelling domain (black), and examples of the nested grids, for 2003 in red, and for 2005 in yellow. The two horizontal white lines in the smallest 2003 domain are the cross-sections at roughly 34 and 39° N described in Sect. 4.3.

ACPD
12, 16557–16602, 2012

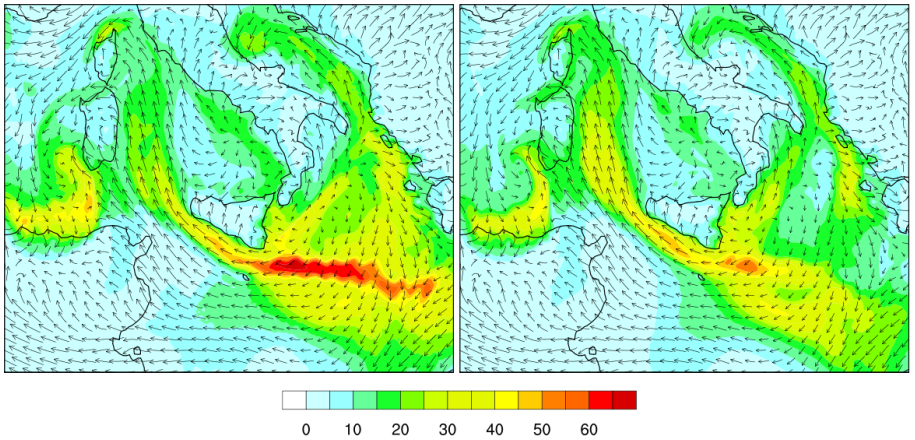

Fig. 3. The influence of ship emission height on the modelled O_3 concentration in ppb, in the lowest model layer at midday on 16 June 2009. Left, Em_low scenario right, Em_hi scenario.

ACPD
12, 16557–16602, 2012

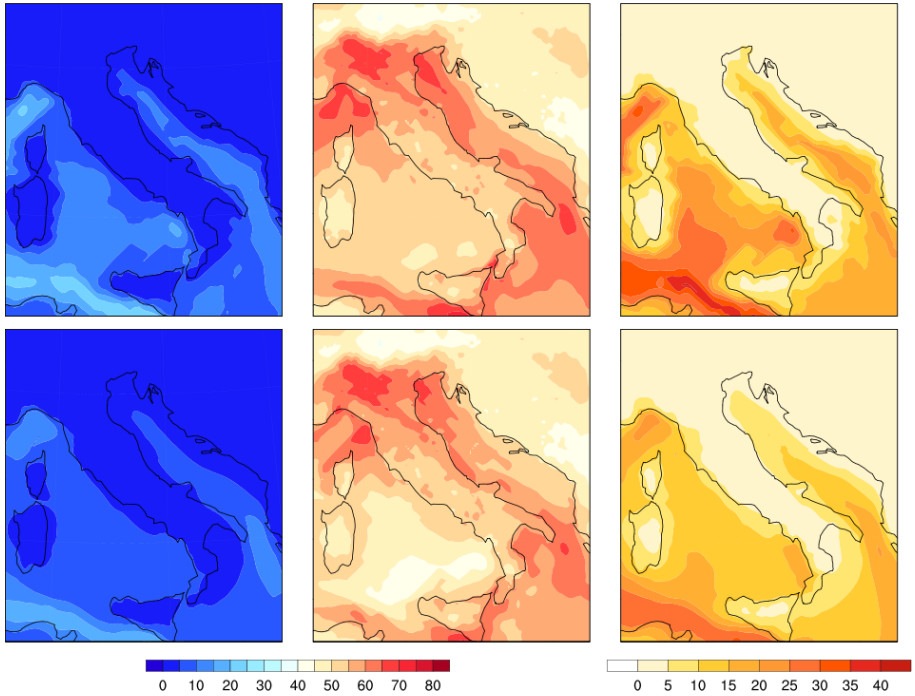

Fig. 4. The O_3 concentration in the first model layer (2005), row one Em_low, row 2 Em_hi. Column 1 shows the difference Tot_Emiss – No_ships in ppb, column 2 the actual value in ppb and column 3 the difference in %. The values are the average for the whole simulation period, 15 June till 29 June.

ACPD
12, 16557–16602, 2012

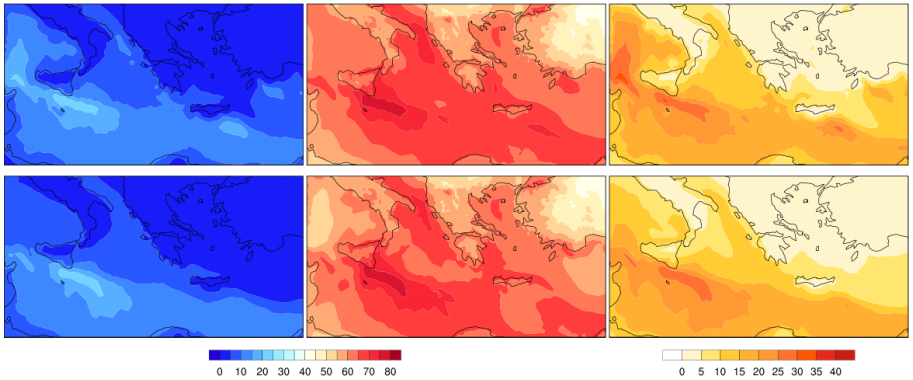

Fig. 5. The O_3 concentration in the first model layer (2006), row one Em_low, row 2 Em_hi. Column 1 shows the difference Tot_Emiss – No_ships in ppb, column 2 the actual value in ppb and column 3 the difference in %. The values are the average for the whole simulation period, 5–20 July.

ACPD
12, 16557–16602, 2012

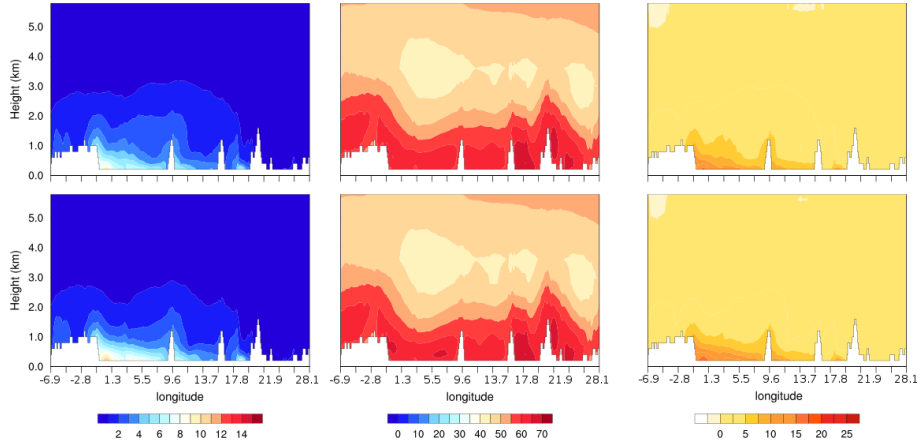

Fig. 6. The vertical profile of O_3 concentration along ≈39° N. Row one Em_low, row 2 Em_hi. Column 1 shows the difference Tot_Emiss – No_ships in ppb, column 2 the actual value in ppb and column 3 the difference in %. The values are the average for the whole simulation period, 5 to 27 August 2003.

ACPD
12, 16557–16602, 2012

Summertime contribution of ship emissions to Mediterranean ozone

I. M. Hedgecock et al.

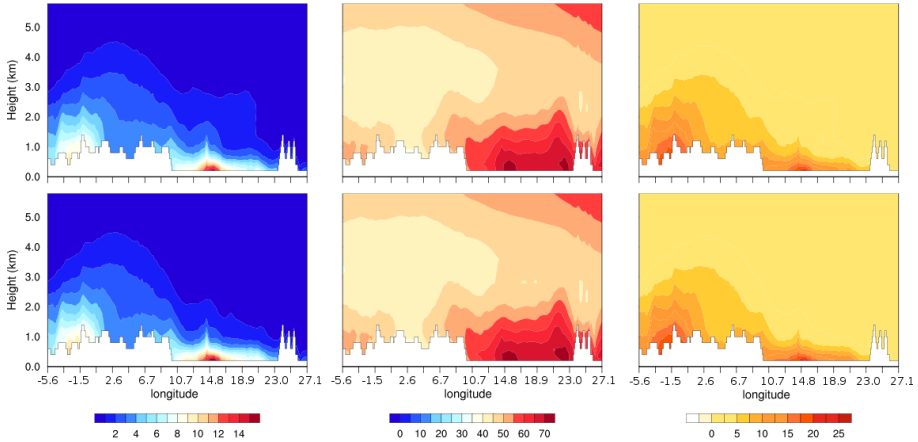

Fig. 7. The vertical profile of O_3 concentration along ≈34° N. Row one Em_low, row 2 Em_hi. Column 1 shows the difference Tot_Emiss – No_ships in ppb, column 2 the actual value in ppb and column 3 the difference in %. The values are the average for the whole simulation period, 5 to 27 August 2003.

ACPD
12, 16557–16602, 2012

Summertime contribution of ship emissions to Mediterranean ozone

I. M. Hedgecock et al.

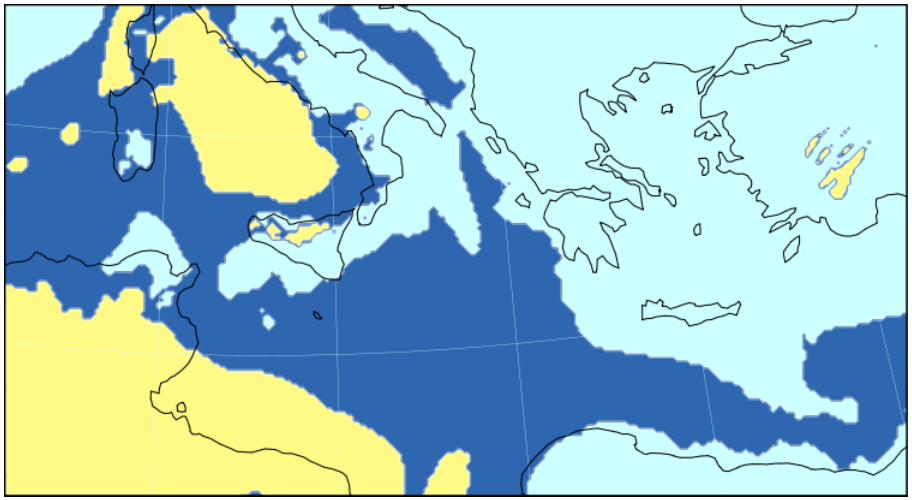

Fig. 8. An example case showing the areas where the model results indicate that ships emissions made difference between complying and not complying to the EU 8 h air quality standard for O_3 of 120 µg m^{-3}. The light blue areas represent regions where the standard is not met in either case, the yellow areas are where the standard is met in both cases and the dark blue is where the standard is not met in the Tot_Emiss simulations but is complied with in the No_ships simulation, 29 July 2000, Em_low scenario.

ACPD
12, 16557–16602, 2012

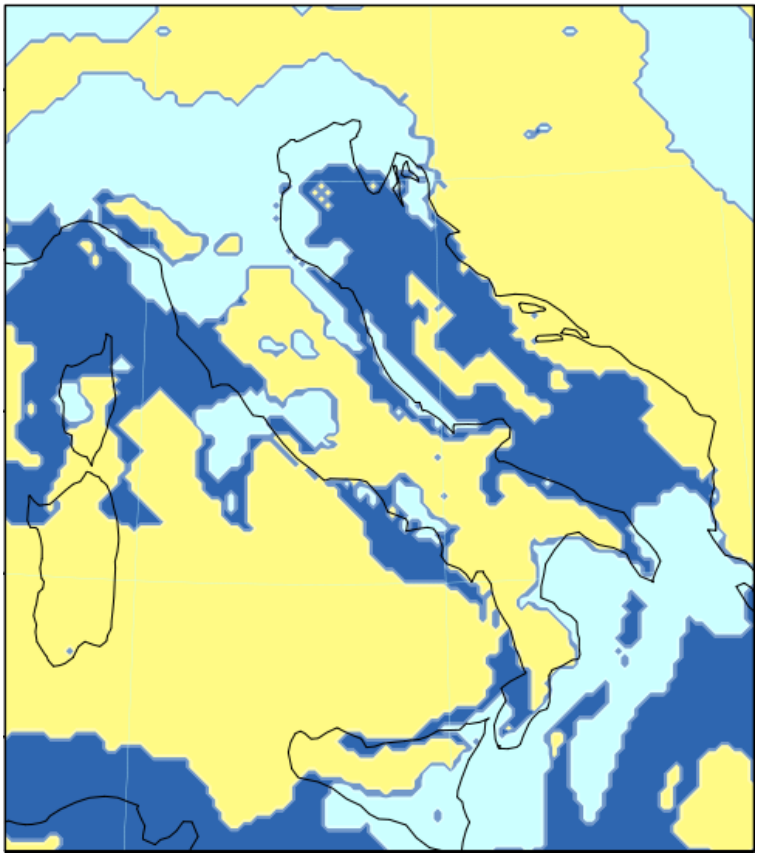

Fig. 9. The areas where the model results indicate that ships emissions made difference between complying and not complying to the EU air quality standard, 21 June 2005, Em_hi scenario. For the significance of the colours, see the caption of Fig. 8.

ACPD
12, 16557–16602, 2012